

# Journal of Materials Chemistry B

Accepted Manuscript



This is an *Accepted Manuscript*, which has been through the Royal Society of Chemistry peer review process and has been accepted for publication.

*Accepted Manuscripts* are published online shortly after acceptance, before technical editing, formatting and proof reading. Using this free service, authors can make their results available to the community, in citable form, before we publish the edited article. We will replace this *Accepted Manuscript* with the edited and formatted *Advance Article* as soon as it is available.

You can find more information about *Accepted Manuscripts* in the [Information for Authors](#).

Please note that technical editing may introduce minor changes to the text and/or graphics, which may alter content. The journal's standard [Terms & Conditions](#) and the [Ethical guidelines](#) still apply. In no event shall the Royal Society of Chemistry be held responsible for any errors or omissions in this *Accepted Manuscript* or any consequences arising from the use of any information it contains.

Cite this: DOI: 10.1039/c0xx00000x

www.rsc.org/xxxxxx

ARTICLE TYPE

# Enzymes as Bionanoreactors: Glucose Oxidase for the Synthesis of Catalytic Au Nanoparticles and Au Nanoparticle-Polyaniline Nanocomposite

Bhagwati Sharma, Sonam Mandani and Tridib K. Sarma\*

5 Received (in XXX, XXX) Xth XXXXXXXXXX 20XX, Accepted Xth XXXXXXXXXX 20XX  
DOI: 10.1039/b000000x

The use of biomaterials such as enzymes for the synthesis of functional materials is important because such biologically guided process can have a significant impact on the reduction of energy consumption in manufacturing processes. Glucose oxidase (GOx) has been exploited as a reducing as well as stabilizing agent for the green chemical synthesis of Au nanoparticles at pH 7.0 under ambient conditions. The synthesized Au nanoparticle-GOx composite was found to act as a highly effective catalyst towards the reduction of *p*-nitrophenol to *p*-aminophenol in presence of NaBH<sub>4</sub>. The catalytic activity of GOx was largely inhibited after its participation in the reduction of metal salt to form nanoparticles. A detailed mechanistic investigation was carried out through fluorescence spectroscopy, Fourier transform infra-red (FTIR) spectroscopy and circular dichroism (CD) to have an insight into the conformational changes in the enzyme structure. The catalytic activity of GOx towards the oxidation of glucose was taken advantage of towards the formation of Au nanoparticle-polyaniline (Au NP-PANI) composite at room temperature. The production of green emeraldine salt form of polyaniline (PANI) was extremely low in case of Au nanoparticle-GOx composite, where GOx was involved as a reducing agent. However, H<sub>2</sub>O<sub>2</sub> generated during the catalytic reaction of GOx acted as a simultaneous reducing as well as oxidizing agent leading to the formation of Au NP-PANI core-shell composite in a controlled fashion.

## Introduction

The assembly of nanoscale objects is considered to be a fundamental step in the building of new functional materials.<sup>1-3</sup> Since structural precision is a must for the optimization of properties and functions of the nanoscale materials, there is a continuous surge in probing self-assembled molecular systems such as molecular and polymeric micelles,<sup>4</sup> porous materials<sup>5</sup> etc. as templates for the precise and directional growth of nano-dimensional systems. The nucleation and growth of the nanoparticles are governed by spatially confined environment and presence of nucleation sites in these templates. Biomolecule templated growth of nanostructured materials has evolved as a magnificent alternative strategy in recent years. Microbes such as viruses,<sup>6</sup> fungi<sup>7</sup> etc. and a variety of biomolecules such as proteins, peptides and nucleic acids have been used as templates for the fabrication and functionalization of inorganic nanostructures.<sup>8-14</sup> Enzymes, responsible for the interconversion of various reactions in the living world, have attracted a tremendous interest in the development of nano-bio integrated materials. The adsorption of enzymes on the nanoparticle surface via chemical or electrostatic attachment might have an effect on the conformational changes in the enzyme structure.<sup>15,16</sup> The resulting alteration of the catalytic functionality of the enzyme or agglomeration of the nanoparticles induced by enzymes have been taken advantage of towards the development of colorimetric

and electrochemical detection pathways for sensing biomolecules.<sup>17-21</sup> On the other hand, the synthesis of metal and metal oxide nanoparticles has been explored during an enzyme catalyzed reaction, where the product of the enzyme stimulated reaction governs the nucleation and growth of the nanoparticles.<sup>22,23</sup> Although, there have been quite a few reports exploring the enzymes as reducing as well as stabilizing agents themselves for the synthesis of metallic nanoparticles,<sup>24-27</sup> a clear detailed mechanistic investigation of reduction of metal salts by enzymes have not been performed. A clear understanding of the reduction capability of enzymes and resulting conformational changes in the native enzyme structure will provide a greener and cheaper alternative towards synthesis of inorganic materials under mild conditions, thus eliminating the conventional drawbacks such as elevated temperature and harsh chemical reagents often used in wet chemical synthetic methodologies. Further, the use of enzymes will also provide a pathway for the development of nanoparticle incorporated functional materials with potential in diverse applications, taking advantage of the activity of the enzyme. In this direction, we have recently established that a commonly available enzyme such as Jack bean urease could be exploited for the synthesis of metals, metallic alloys and metal-semiconductor core-shell nanostructures.<sup>25</sup> Among the conducting polymers, polyaniline (PANI) is one of the most extensively studied because of its high environmental

stability and tunability of opto-electrical properties.<sup>28,29</sup> The beauty with PANI is that on one hand it has optical, electronic and magnetic properties that could be tailored from metallic to insulator depending on its oxidation state and degree of protonation and on the other hand it shows property of flexibility and processability characteristic of conventional polymers.<sup>30</sup> PANI offers the added advantage that unlike other conjugated polymers it has a simple and reversible acid/base doping/dedoping chemistry<sup>31</sup> which enables control over physico-chemical properties such as electrical conductivity, optical activity etc. and has attracted immense technological importance. Further, composite materials of PANI with metal nanoparticles are currently of great research interest as they combine the tunable opto-electronic properties of this low dimensional organic conductor with unique optical and catalytic properties of metallic nanoclusters. Therefore, there has been a great surge for synthetic methodologies involving single reagent for the generation of metallic nanoparticles as well as polymerization of aniline, thereby resulting in a composite.<sup>32-36</sup> The major concern of dispersibility as well as processability of PANI in common solvents could be overcome by controlling the size of the composite in the nanometer dimension. The use of bioreactors with spatially confined environment such as enzymes could provide an environmentally favourable pathway towards the controlled generation of biofunctionalized nanoparticle-PANI composites in water under mild conditions.

Herein, we report a simple, green and efficient synthesis of Au NPs as well as Au NP- PANI nanocomposite using the enzyme glucose oxidase. Glucose oxidase, a flavoprotein, is a dimer of two identical monomer units with molecular mass of 160 kDa. The enzyme contains one flavin adenine dinucleotide (FAD) molecule, one free sulfhydryl group<sup>37</sup> and several other free amino acid residues per monomer, with known reduction capability for Au<sup>3+</sup> ions to form Au-NPs. The nanoparticles synthesized using GOx exhibited excellent catalytic activity towards the reduction of *p*-nitrophenol to *p*-aminophenol, with NaBH<sub>4</sub> acting as a reducing agent. GOx was investigated as reducing as well as stabilizing agent for the synthesis of Au NPs because it is a redox enzyme and is involved in the breakdown of D-glucose to gluconic acid and H<sub>2</sub>O<sub>2</sub>. The byproduct H<sub>2</sub>O<sub>2</sub> is well known to polymerize aniline into PANI.<sup>32</sup> So we anticipated that after the synthesis of Au NPs, the enzyme activity might be capitalized to polymerize aniline, thereby resulting in Au NP-PANI nanocomposite. However, the enzyme activity was largely inhibited after it was involved in the reduction of Au<sup>3+</sup> to form Au NPs. Therefore, in an alternative strategy, the Au NP-PANI composite was synthesized with controlled dimension in a glucose oxidase stimulated pathway, where the H<sub>2</sub>O<sub>2</sub> generated during the oxidation of glucose was used as both reducing as well as oxidizing agent.<sup>32</sup> It was interesting to note that the PANI as well as Au NP-PANI nanocomposite synthesized using GOx were well dispersed in water and stable without any signs of precipitation.

## Experimental Section

### Materials

Glucose oxidase from *Aspergillus niger*, hydrogen

tetrachloroaurate and 5,5'- dithiobis(2-nitrobenzoic acid) (DTNB), were purchased from Sigma-Aldrich. Sorbitol and xylenol orange were purchased from SRL chemicals, India. Sodium dihydrogen phosphate monohydrate, di- Sodium hydrogen phosphate, glucose, ferrous ammonium sulfate and hydrochloric acid were purchased from Merck, India. Aniline was purchased from Merck, India and was distilled under vacuum prior to use. All the reagents were of analytical grade and were used without any further purification. Milli Q water was used throughout the experiments.

### Synthesis of Au nanoparticles

Au nanoparticles were synthesized in Phosphate buffer of strength 10 mM and pH 7.0. Briefly, HAuCl<sub>4</sub> solution with a final concentration of  $6 \times 10^{-4}$  M was added to 3 ml of 0.7 mg/ml glucose oxidase solution in phosphate buffer and the reaction was incubated at 37 °C for 36 hours with mild stirring, when the color of the solution changed from light yellow to pink.

### Catalytic activity of Au nanoparticles

The catalytic activity of the Au NP-enzyme composite was tested by carrying out the reduction of *p*-nitrophenol to *p*-aminophenol using NaBH<sub>4</sub> as the reducing agent. To a standard quartz cell of 1 cm pathlength, 2.5 ml of 0.12 mM *p*-nitrophenol, 1 mg NaBH<sub>4</sub> and 0.025 ml of as prepared Au nanoparticles was added and the UV-visible spectra were recorded every 2 minutes in the range of 200-600 nm.

### Circular Dichroism Studies

Circular Dichroism (CD) measurements were performed at 25 °C on a JASCO J-815 spectropolarimeter. All the spectra were recorded with a data pitch of 0.1 nm. The scanning speed was set to 20 nm/min with band width of 1nm. For the far UV region (190-250 nm), spectra were recorded with an enzyme concentration of 0.7 mg/ml using a quartz cell of 1mm pathlength (Starna Scientific Ltd. Hainault, UK). For the near UV and visible region (250-450 nm) we used an enzyme concentration of 1.85 mg/ml and the measurements were performed in a 1cm pathlength cell (Hellma Analytics). Each spectrum is the result of average of three consecutive scans.

### Synthesis of Au nanoparticle-polyaniline nanocomposite

Au nanoparticle-polyaniline nanocomposite was synthesized employing the activity of glucose oxidase. To 3.2 ml of 1.25 mg/ml enzyme solution in PBS of pH 7.0, 70 mg of glucose was added under mild stirring. After 2 minutes 50 µl of 0.03 M HAuCl<sub>4</sub> was added that resulted in the formation of Au nanoparticles within 3 minutes. To this solution, 100 µl of distilled aniline in 2.5 ml of 1 M HCl was added drop wise and the reaction mixture was stirred at room temperature for 16 hours, resulting in a dark green coloured solution.

## Results and Discussion

The reducing capability of GOx was realized by the incubation

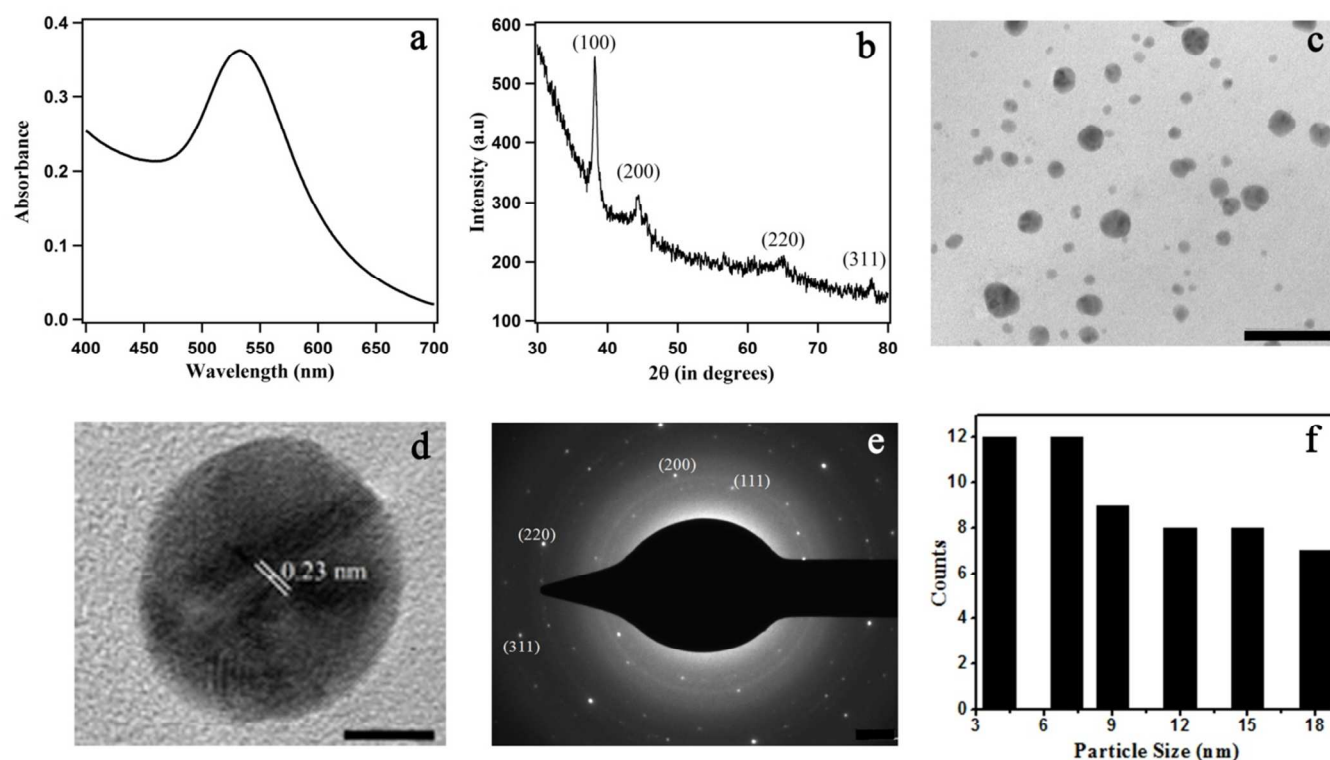


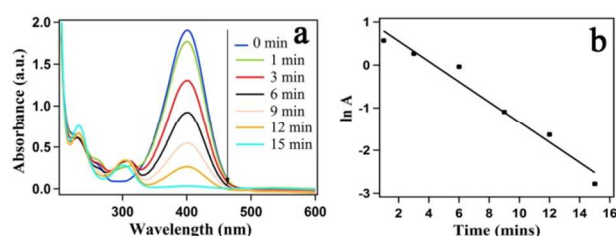
**Fig. 1** (a) UV-visible spectrum of Au nanoparticles synthesized using glucose oxidase. (b) Powder XRD spectrum of Au nanoparticles showing characteristic Bragg peaks. (c) TEM image of Au nanoparticles; scale bar 50 nm. (d) HRTEM image of Au nanoparticles showing lattice separation corresponding to (111) plane of Au; scale bar 5 nm. (e) SAED pattern of the Au nanoparticles; scale bar 2.00 1/nm and (f) particle size distribution of Au nanoparticles.

of the enzyme (3 ml of 0.7 mg/ml) with  $\text{HAuCl}_4$  (final concentration of  $6 \times 10^{-4}$  M) in phosphate buffer saline (PBS) at pH 7.0 and 37°C. The simple incubation resulted in a colour change from light yellow to pink after 36 hours (Figure S1), which colorimetrically indicated the formation of Au NPs. The synthesized Au NPs exhibited their characteristic surface plasmon resonance (SPR) band at 533 nm (Figure 1a). The powder XRD spectrum consisted of peaks at  $2\theta$  values of 38.2, 44.4, 64.6 and 77.7 degrees corresponding to (111), (200), (220) and (311) facets of the fcc structure of Au (Figure 1b). The TEM image (Figure 1c) showed nearly spherical particles, and from the particle size histogram it was observed that the diameter varied from 3-18 nm and the average particle size was calculated to be  $9.9 \pm 4.3$  nm. The average crystallite size of 11.5 nm as calculated from the Scherrer equation was in good agreement with the TEM results. The average particle size of Au NPs (as calculated from TEM images) correlated well with the optical properties of the nanoparticles as predicted by theoretical calculations (Figure S2) and previous experimental reports.<sup>38,39</sup> The HRTEM image of Au NPs as shown in figure 1d indicated the presence of planes with lattice spacing 0.23 nm due to the (111) plane of Au. Selected area electron diffraction (SAED) pattern of the Au nanoparticles (Figure 1e) further confirmed their crystallinity and was well in accordance with the powder XRD data. It is important to note that the glucose oxidase: $\text{HAuCl}_4$  ratio played a crucial role in controlling the Au nanoparticle size and stability. When we performed the synthesis of Au nanoparticles by varying the concentration of both the

enzyme and gold salt under the similar reaction conditions, we observed drastic changes in the nanoparticle structure and agglomeration. It was observed that when the concentration of the enzyme was increased by 2.5 times (1.75 mg/ml), keeping the concentration of  $\text{HAuCl}_4$  constant (i.e.  $6 \times 10^{-4}$  M), the Au nanoparticles agglomerated to form flower like structure (Figure S3). When the concentration of enzyme was kept constant (0.7 mg/ml) and the concentration of  $\text{HAuCl}_4$  was increased to 2.5 times (final concentration  $1.5 \times 10^{-4}$  M) and 5 times (final concentration  $3 \times 10^{-4}$  M), it was observed that the particles agglomerated to give a flower like morphology (Figure S4) and worm like morphology (Figure S5) respectively.

Metallic NPs deposited on various support systems such as polymers,<sup>40,41</sup> peptides,<sup>42,43</sup> inorganic oxides<sup>44,45</sup> etc. have shown tremendous applicability as heterogeneous catalysts. In order to realize the catalytic potential of Au NPs on an enzyme support, we carried out the reduction of *p*-nitrophenol in water using  $\text{NaBH}_4$  as the reducing agent. The reduction of *p*-nitrophenol by  $\text{NaBH}_4$  was chosen as a model reaction because the progress of the reaction can easily be monitored using UV-visible spectroscopy. The addition of  $\text{NaBH}_4$  to a *p*-nitrophenol solution resulted in the change in color of the solution from light yellow to intense yellow due to the formation of *p*-nitrophenolate ion. In absence of Au NPs the reduction leading to the formation of *p*-aminophenol did not occur at all even after 4 days. This was evident through the control experiments, which showed only a single peak at 400 nm in the UV-visible spectrum as attributed to the *p*-nitrophenolate ion (Figure S6). However, with the addition

of Au NP-GOx composite, the yellow colour of the solution slowly faded away, as confirmed visually (Figure S7). UV-visible studies showed a gradual decrease in the intensity of the peak at 400 nm and formation of a new peak at 300 nm (Figure 2a),  
 5 indicative of the gradual conversion of *p*-nitrophenolate ion to *p*-aminophenol. The Au NP-GOx composite was found to act as a highly effective catalyst as evidenced by the reduction of 0.12 mM *p*-nitrophenol in just 15 minutes, when 25  $\mu$ l of the Au nanoparticle-GOx composite was used as catalyst ( $\sim$  0.005 mmol).  
 10 Controlled experiment with solution of *p*-nitrophenol containing GOx without Au NPs was also performed to ascertain that it was the Au NPs rather than GOx which acted as a catalyst. It was confirmed from the controlled experiment that GOx alone was incapable of catalyzing the reduction, as the color of the  
 15 solution remained unaltered even after a week. Since for the reduction a large excess of  $\text{NaBH}_4$  was used, it was reasonable to consider its concentration to be constant throughout the reaction and the kinetics of the reaction could be evaluated with respect to the rate of *p*-nitrophenol consumption. A linear relationship  
 20 between  $\ln$  (absorbance) and time (Figure 2b) was indicative of pseudo first order kinetics. The apparent rate constant,  $k$  as calculated from the plot of  $\ln A$  versus time was found to be  $4.2 \times 10^{-3} \text{ s}^{-1}$ .



25 **Fig.2** (a) Time dependent UV-Visible spectra for the catalytic reduction of *p*-nitrophenol by  $\text{NaBH}_4$  in the presence of Au nanoparticles synthesized using glucose oxidase. (b) plot of natural log of absorbance at 400 nm versus time. The value of apparent rate constant  $k$  as calculated from the slope in (b) is  $4.2 \times 10^{-3} \text{ s}^{-1}$ .

30 To elucidate the activity of the enzyme post the reduction of  $\text{Au}^{3+}$  to Au NPs, we attempted the synthesis of PANI using the Au NP-enzyme composite. For this, glucose was added to the Au NP-GOx solution followed by addition of aniline in HCl (pH of the final solution was 2.0). In case of active GOx, glucose should  
 35 have been converted to gluconic acid and  $\text{H}_2\text{O}_2$ , and the  $\text{H}_2\text{O}_2$  formed should have acted as an oxidant for the polymerization of aniline leading to the formation of green emeraldine salt form of PANI. However, there was only a slight change in the colour of the solution and the typical green colour of emeraldine salt form  
 40 was not observed. The UV-visible spectrum showed a small peak at 738 nm along with a much intense peak at 536 nm corresponding to Au NPs (Figure S8). This indicated that  $\text{H}_2\text{O}_2$  generation by GOx in this case was extremely low. From this experiment it was concluded that the enzymatic activity of GOx  
 45 was largely inhibited after their participation as a reducing agent for the synthesis of Au NPs. The decrease in the activity of the enzyme was further confirmed by the spectrophotometric assay based on the oxidation of ferrous ions by  $\text{H}_2\text{O}_2$  in the presence of xylenol orange, known as FOX method (Figures S9 and S10).

50 The decrease in the activity of the enzyme is attributed to the

conformational change that the enzyme had undergone during the synthesis of Au NPs. Circular Dichroism (CD) is a major tool for studies related to the conformational changes in a protein. Secondary and tertiary structural changes in the enzyme can be  
 55 followed by observing the changes in the CD signals at particular wavelengths.<sup>46</sup> So, CD was used to probe the changes in the conformation of glucose oxidase after the synthesis of Au NPs. The native enzyme exhibited characteristic minima at around 208 nm and 222 nm in the far UV region (Figure 3a), a strong band in the  
 60 near UV region at 274 nm and another CD band due to flavin adenine dinucleotide (FAD) in the visible region at 375 nm (Figure 3b). However in case of GOx after the synthesis of Au NPs, the CD band at 222 nm decreased in intensity and the minima at 208 nm was shifted to 206 nm together with a decrease  
 65 in the intensity. The results signify a decrease in the  $\alpha$ -helical content of the enzyme which is an indication of changes in its secondary structure. In the near UV region, the intense CD band at 274 nm that arises due to the asymmetric environment of the aromatic amino acid residues disappeared completely suggesting  
 70 the perturbation in the tertiary structure of the enzyme.<sup>47</sup> Also it was found that the band at 375 nm drastically decreased in intensity and was shifted to 333 nm. The change in environment around the FAD during the synthesis of Au NPs may probably be the reason for such a shift and decrease in intensity.<sup>47</sup>

75 In order to ascertain that the variations observed in CD spectrum of GOx after the synthesis of Au NPs were due to the conformational changes taking place during their involvement in the reduction of  $\text{Au}^{3+}$  to  $\text{Au}^0$ , we performed the CD investigation of GOx adsorbed on Au NPs synthesized by citrate method. The  
 80 Au NPs synthesized using trisodium citrate as a reducing agent were incubated with GOx for 12 hours to allow its adsorption on the surface of nanoparticles. As observed from the CD spectra in the UV and visible region, there were no appreciable changes in the characteristic bands, signifying that the secondary and tertiary  
 85 structure of GOx were intact after getting adsorbed on Au NPs. This was further confirmed by the polymerization of aniline in presence of glucose, where the green Au NP-PANI composite was formed (Figure S11).

The conformational changes in the enzyme structure were  
 90 further confirmed using FTIR spectroscopy. FTIR spectrum in the region of  $1700\text{-}1600 \text{ cm}^{-1}$  and  $1600\text{-}1500 \text{ cm}^{-1}$  known as amide I and amide II region respectively yielded useful information about the conformational changes in the enzyme secondary structure. The FTIR spectrum of native GOx and Au  
 95 NP-GOx composite is shown in figure 3c. It was observed that the position of the amide I band in the enzyme was shifted from  $1641 \text{ cm}^{-1}$  to  $1644 \text{ cm}^{-1}$ , whereas the amide II band at  $1548 \text{ cm}^{-1}$  in native GOx almost completely disappeared after the synthesis of Au NPs by the enzyme and was shifted to  $1552 \text{ cm}^{-1}$ , signifying  
 100 perturbation in the secondary structure of the enzyme, consistent with the CD results.

Enzymes are composed of various amino acid residues, whose arrangement into sheets or helices accounts for their complex structures and activity. It has been reported that the free and  
 105 exposed thiol groups in cysteine have the capability for the reduction of metal salts to nanoparticles because of the higher affinity of thiols for the metals.<sup>48</sup> Since GOx dimer contains two free sulphhydryl groups, we assumed that these groups were

responsible for the reduction of  $\text{Au}^{3+}$  to  $\text{Au}^0$ . To support our assumption, we modified the sulfhydryl groups in GOx using 5,5'-dithiobis(2-nitrobenzoic acid) (DTNB). The addition of  $\text{HAuCl}_4$  to the DTNB modified enzyme did not result in the formation of Au NPs, as evidenced visually and from UV-visible studies (Figures S12 and S13), which showed the absence of SPR band of Au NPs. Further, FTIR studies showed the absence of a weak band at  $2630\text{ cm}^{-1}$  attributed to the S-H stretching<sup>49</sup> in the Au NP-GOx composite (Figure S14), confirming the oxidation of the free sulfhydryl group during Au NP synthesis. In case of heat denatured GOx, the incubation of  $\text{HAuCl}_4$  led to the formation of Au NPs in an approximately similar duration as that of the native enzyme, clearly depicting the fact that it is not the native three dimensional structure of GOx but the functional groups present in it which are essential for the Au NP synthesis.

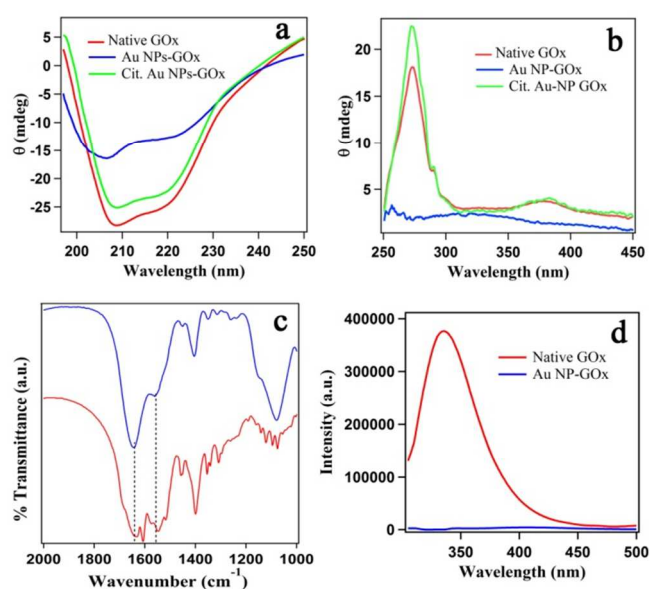


**Fig 3.** Circular dichroism spectrum of glucose oxidase and Au nanoparticle-glucose oxidase composite in (a) far UV region and (b) near UV and visible region. (Red line, native enzyme; Blue line, Au NP-GOx composite; Green line, Citrate capped Au NP-GOx composite). (c) FTIR spectrum of native glucose oxidase (red line) and Au nanoparticle-glucose oxidase composite (blue line). (Dashed lines indicate the shift in the amide I and amide II bands in native GOx and Au NP-GOx composite.). (d) Emission spectrum of GOx and Au NP-GOx composite. ( $\lambda_{\text{exc}}=295\text{ nm}$ ).

As the free cysteine group is located away from the FAD active site or glycosylation site, we expected that modification of the cysteine groups will not have any impact on the catalytic activity of the enzyme after they participated in the reduction of the metal salt.<sup>24</sup> However, in case of GOx, we observed a large inhibition of enzymatic activity after their involvement in Au NP synthesis. As observed from the CD experiments, there was a drastic conformational change in the FAD active site after the reduction process and subsequent adsorption on the nanoparticle surface. Hence, there is a possibility of involvement of other amino acids in the active site or FAD itself in the stabilization of nanoparticles. From the CD spectrum, we observed that the band at  $274\text{ nm}$  in case of native GOx was absent after the synthesis of Au NPs. As the band signifies the asymmetric environment of the

aromatic amino acid residues, its absence suggested the possibility of the involvement of amino acids such as tryptophan, tyrosine and phenylalanine in the reduction/stabilization process. Fluorescence studies further revealed the probable involvement of tryptophan residues in the reduction of  $\text{Au}^{3+}$  to  $\text{Au}^0$ . In the fluorescence spectrum as shown in figure 3d, it was observed that upon excitation at  $295\text{ nm}$  the native enzyme exhibited emission at  $335\text{ nm}$  with a sufficiently high intensity. However after the synthesis of Au NPs, the emission at  $335\text{ nm}$  was completely quenched, suggesting the probable loss or modification of the tryptophan residues. Previous report<sup>47</sup> have shown that in case of native enzyme, the emission intensity originating due to tryptophan residues in GOx is significantly lower due to Forster resonance energy transfer from the tryptophan residues to FAD. However, in case of heat denatured enzyme, the emission peak corresponding to tryptophan enhances significantly as FAD is dissociated from GOx in this case. However, in our case the fluorescence due to the tryptophan residues was completely quenched after the synthesis of Au NPs, suggesting their possible involvement in the reduction or capping of the nanoparticles. Nevertheless, a clear understanding of the mechanism for the biogenic reduction of metal salt by GOx remains unclear and needs further investigations.

Due to conformational changes in the native structure of the GOx during the formation of Au NPs, the enzyme lost a large fraction of its catalytic activity towards the oxidation of glucose forming gluconic acid and  $\text{H}_2\text{O}_2$ . The Au-GOx composite thus formed was incapable of complete polymerization of aniline leading to the formation of Au NP-PANI composite. Therefore it became imperative for us to look for an alternative strategy for the biocatalytic synthesis of Au NP-PANI composite using GOx as the template. It is well known that  $\text{H}_2\text{O}_2$  has both oxidation and reduction properties.<sup>32</sup> Hence  $\text{H}_2\text{O}_2$  generated through the oxidation of glucose by GOx could be used for the reduction of  $\text{HAuCl}_4$  to form Au NPs followed by oxidative polymerization of aniline in a one-pot synthesis leading to Au NP-PANI composite material with nanometer dimension.

The time dependent formation of Au NP-PANI nanocomposite was followed by UV-visible spectroscopy and the results are shown in figure 4a.  $\text{H}_2\text{O}_2$  generated by the catalytic oxidation of glucose by GOx was able to reduce  $\text{HAuCl}_4$  to form Au NPs that showed purple color and exhibited SPR band at  $562\text{ nm}$  (Figure S16). However upon the addition of HCl, the colour of the solution changed to pink within 30 minutes and the SPR band blue shifted to  $537\text{ nm}$ . It is known that nanoparticles are very sensitive to the dielectric constant of the surrounding environment and a slight change in the medium can result in a marked variation in the position and intensity of the SPR band.<sup>50,51</sup> In the present case, the change of dielectric constant upon change of pH from 7.0 to 2.0 probably caused the SPR band of Au NPs to shift from  $562\text{ nm}$  to  $537\text{ nm}$ . When aniline was added, the intensity of the SPR band of Au NPs at  $537\text{ nm}$  first increased but began to decrease as the aniline started to polymerize. With time, the colour of the solution became light green to dark green suggesting the formation of the conductive emeraldine salt form of PANI, with the continuous growth of two new peaks at  $360\text{ nm}$  and  $735\text{ nm}$  in the UV-visible spectra. The decrease in the intensity of the Au SPR band at  $537\text{ nm}$  could be

attributed to the PANI coating on the Au NPs. It was observed that the SPR band of Au NPs, though decreased in intensity with time, but was clearly evident in the UV-visible spectrum even after complete polymerization of aniline. Previously, it was reported that the plasmon resonance band of Au NPs disappeared while they were exposed to positively charged anilinium ions, hence optical characteristics of Au NPs could not be observed in the Au NP-PANI composite.<sup>32,33</sup> In our case, the Au NPs formed as a result of the reduction of HAuCl<sub>4</sub> by H<sub>2</sub>O<sub>2</sub> were stabilized by the enzyme. Thus the enzyme layer on the nanoparticle surface prevented the direct interaction of Au NPs with the positively charged anilinium ions. As a result of this, the SPR band of the Au NPs was evident in the composite. For comparison, we also synthesized PANI nanoparticles by the same synthetic pathway in absence of Au NPs. In this case, the longitudinal band of PANI was observed at 755 nm, a 20 nm shift towards the longer wavelength as compared to Au NP-PANI composite (Figure S17). The shift might be due to the formation of PANI of a molecular weight different from that of the composite or it might also be a signature of the level of proton doping in the PANI synthesized in the absence of Au NPs.<sup>33</sup>

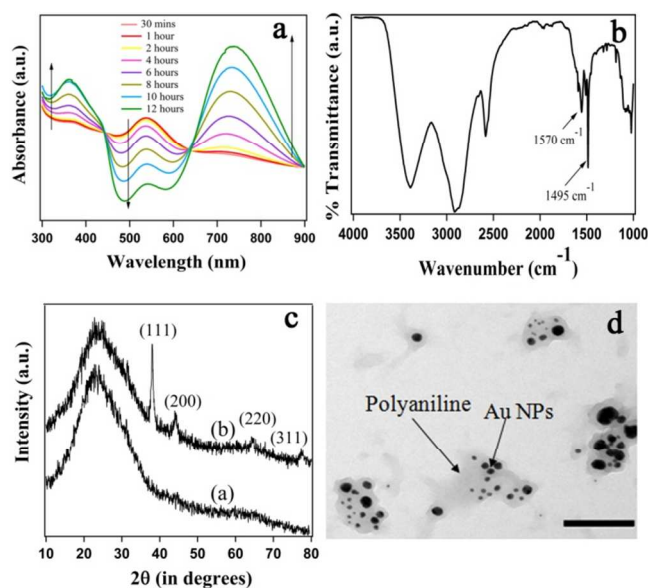


**Fig 4.** (a) Time dependent UV-visible spectrum of Au nanoparticle-polyaniline nanocomposite synthesized using glucose oxidase. (b) FTIR spectrum of Au nanoparticle-polyaniline composite. (c) Powder XRD pattern of (a) Polyaniline alone and (b) Au nanoparticle-polyaniline nanocomposite and (d) TEM image of Au nanoparticle-polyaniline nanocomposite; scale bar 200 nm.

The FTIR spectrum of the Au NP-PANI nanocomposite (Figure 4b) showed peaks at 1495 and 1570 cm<sup>-1</sup> which are characteristic of the benzenoid and quinoid ring deformations respectively. The broad peak at 3400 cm<sup>-1</sup> is assigned to N-H stretching. This spectrum was quite similar to the spectrum of PANI synthesized by the same procedure but in the absence of Au NPs (Figure S18), which suggested that there was little structural difference between the PANI alone and PANI in the Au NP-PANI composite. In both the cases, the benzenoid band at 1495 cm<sup>-1</sup> was more intense than the quinoid band. The electrochemical nature of the PANI in the Au NP-PANI

nanocomposite was evaluated by cyclic voltammetry (Figure S19). Generally two sets of redox peaks are observed in case of PANI. However in our case the Au NP-PANI composite showed only one set of redox peak at E<sub>1/2</sub> = 0.45 V. The absence of the second redox process may be attributed to the exceptional resistance of PANI to oxidation to pernigraniline state, as has been reported earlier.<sup>52</sup>

The incorporation of Au NPs in the PANI moiety was established using powder XRD and transmission electron microscopy. The powder XRD spectrum (Figure 4c) in case of PANI alone consisted of only a broad peak at 2θ value of 23.8° indicating that low level of crystalline phase in the polymer had been formed.<sup>33</sup> However in case of the Au NP-PANI composite, in addition to the broad peak at 24°, peaks at 2θ values of 38.2, 44.5, 64.7 and 77.6 degrees corresponding to (111), (200), (222), and (311) planes of Au were observed, confirming the presence of Au nanoparticles along with the polymer. The transmission electron microscopy image (Figure 4d) of the Au NP-PANI composite revealed that the Au NPs were mostly in the form of a cluster of particles surrounded by a layer of PANI. The clusters were well separated from each other and the average size of each cluster was around 100 nm. The Au NP-PANI composite appeared to have a core-shell morphology where the cluster of the particles formed the core and the surrounding PANI layer formed the shell. The Au NPs and PANI in the Au NP-PANI composite were clearly distinguishable from each other where the Au NPs formed the dark core and the PANI layer was observed as light gray shell. It was also observed that in some cases even a single Au NP could be encapsulated in the PANI shell (Figure S20). The average particle size of Au nanoparticles were found to be 14.1 ± 6.4 nm. The corresponding EDS spectrum (Figure S21) showed the presence of carbon, nitrogen and Au confirming the presence of Au NPs in the PANI matrix.

## Conclusions

In conclusion, we have developed a simple and green method for the synthesis of Au NPs using a redox enzyme, glucose oxidase as both reducing as well as stabilizing agent. The synthesized Au nanoparticles showed excellent catalytic activity towards the reduction of *p*-nitrophenol to *p*-aminophenol. The use of enzymes for the synthesis of metal nanoparticles is important not only towards the development of biogenic pathway devoid of harsh reaction conditions, but also because it may provide an insight into the mechanism of nanoparticle formation in higher ordered organisms such as fungi, bacteria, viruses etc. With an enhanced role of opto-electronic properties of Au nanoparticles and their interaction with biomolecules such as enzymes in nanobiotechnology, fundamental understanding regarding the factors which lead to the property changes in either one or both of them are crucial in development of functional materials for applications such as ultrasensitive optical and electrochemical nanosensors.<sup>17-21</sup> Further the catalytic activity of glucose oxidase was exploited towards the formation of Au NP-polyaniline nanocomposite. With the tremendous potential of nanoparticle incorporated conducting polymer composite materials in various applications, development of this biogenic route using enzymes as templates under ambient conditions will offer a green alternative towards the formation of nanocomposite materials.

## Acknowledgements

This work is supported by SERB, DST India research project No. SR/S1/PC-32/2010. B. S. and S. M. acknowledge the research fellowships from UGC (India) and CSIR (India) respectively. We acknowledge the help from Department of Physics, University of Pune, SAIF, NEHU, Shillong and AMRC, IIT Mandi for TEM facility and UGC-DAE consortium for scientific research, Indore for powder XRD facility. We thank Dr. Subrata Ghosh for technical support.

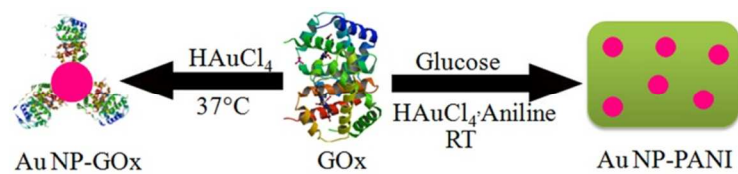
## Notes and references

Discipline of Chemistry, School of Basic Sciences, Indian Institute of Technology Indore, IET Campus-DAVV, Khandwa Road, Indore-452017, India. Tel: +91-731-2438706; E-mail: tridib@iiti.ac.in

Supplementary Information (ESI) available: Additional experimental procedures, reactions and additional spectroscopic data. See DOI: 10.1039/b000000x/

- 1 M. C. Daniel and D. Astruc, *Chem. Rev.*, 2004, **104**, 293-346.
- 2 R. Costi, A. E. Saunders and U. Banin, *Angew. Chem. Int. Ed.*, 2010, **49**, 4878-4897.
- 3 H. Goesmann and C. Feldmann, *Angew. Chem. Int. Ed.*, 2010, **49**, 1362-1395.
- 4 P. Khullar, V. Singh, A. Mahal, H. Kaur, V. Singh, T. S. Banipal, G. Kaur and M. S. Bakshi, *J. Phys. Chem. C*, 2011, **115**, 10442-10454.
- 5 A. Fischer, J. O. Muller, M. Antonietti and A. Thomas, *ACS Nano*, 2008, **2**, 2489-2496.
- 6 J. M. Slocik, R. R. Naik, M. O. Stone, and D. W. Wright, *J. Mater. Chem.*, 2005, **15**, 749-753.
- 7 A. Ahmad, P. Mukherjee, D. Mandal, S. Senapati, M. I. Khan, R. Kumar, and M. Sastry, *J. Am. Chem. Soc.*, 2002, **124**, 12108-12109.
- 8 L. Berti, and G. A. Burley, *Nat. Nanotechnol.*, 2008, **3**, 81-87.
- 9 N. Ma, E. H. Sargent, and S. O. Kelley, *Nat. Nanotechnol.*, 2009, **4**, 121-125.
- 10 H. Wei, Z. Wang, J. Zhang, S. House, Y. G. Gao, L. Yang, H. Robinson, L. H. Tan, H. Xing, C. Hou, I. M. Robertson, J. M. Zhuo and Y. Lu, *Nat. Nanotechnol.*, 2011, **6**, 93-97.
- 11 C. M. Niemeyer, *Angew. Chem. Int. Ed.*, 2001, **40**, 4128-4158.
- 12 L. A. Gugliotti, D. L. Feldheim and B. E. Eaton, *Science*, 2004, **304**, 850-852.
- 13 L. Rodriguez-Lorenzo, R. de la Rica, A. Alvarez-Puebla, L. M. Liz-Marzan and M. M. Stevens, *Nat. Mater.*, 2012, **11**, 604-607.
- 14 M. B. Dickerson, K. H. Sandhage and R. R. Naik, *Chem. Rev.*, 2008, **108**, 4935-4978.
- 15 R. Ghosh, J. Deka, A. Chattopadhyay and A. Paul, *RSC Adv.*, 2013, **3**, 23015-23027.
- 16 C. C. You, M. De, G. Han and V. M. Rotello, *J. Am. Chem. Soc.*, 2005, **127**, 12873-12881.
- 17 M. Zayats, R. Baron, I. Popov and I. Willner, *Nano Lett.*, 2005, **5**, 21-25.
- 18 X. Xu, M. S. Han and C. A. Mirkin, *Angew. Chem. Int. Ed.*, 2007, **46**, 3468-3470.
- 19 X. Xie, W. Xu and X. Liu, *Acc. Chem. Res.*, 2012, **45**, 1511-1520.
- 20 J. Oishi, Y. Asami, T. Mori, J. H. Kang, M. Tanabe, T. Niidome and Y. Katayama, *ChemBioChem*, 2007, **8**, 875-879.
- 21 D. Zhai, B. Liu, Y. Shi, L. Pan, Y. Wang, W. Li, R. Zhang and G. Yu, *ACS Nano*, 2013, **7**, 3540-3546.
- 22 B. Bansar, Y. Weizmann, Z. Cheglakov and I. Willner, *Adv. Mater.*, 2006, **18**, 713-718.
- 23 R. de La Rica and H. Matsui, *Angew. Chem. Int. Ed.*, 2008, **47**, 5415-5417.
- 24 A. Rangnekar, T. K. Sarma, A. K. Singh, J. Deka, A. Ramesh and A. Chattopadhyay, *Langmuir*, 2007, **23**, 5700-5706.
- 25 B. Sharma, S. Mandani and T. K. Sarma, *Sci. Rep.* 2013, **3**, 2601; DOI:10.1038/srep0260.
- 26 S. J. Lee, N. Scotti, N. Ravasio, I. S. Chung and H. Song, *Cryst. Growth Des.*, 2013, **13**, 4131-4137.
- 27 P. Zhang, X. X. Yang, Y. Wang, N. W. Zhao, Z. H. Xiong and C. Z. Huang, *Nanoscale*, 2014, **6**, 2261-2269.
- 28 G. Gustafsson, Y. Cao, G. M. Treacy, F. Klavetter, N. Colaneri and A. J. Heeger, *Nature*, 1992, **357**, 477-479.
- 29 H. Xia, and Q. Wang, *Chem. Mater.*, 2002, **14**, 2158-2165.
- 30 M. Zhao, X. Wu and C. Cai, *J. Phys. Chem. C*, 2009, **113**, 4987-4996.
- 31 J. Huang, S. Virji, B. H. Weiller and R. B. Kaner, *J. Am. Chem. Soc.*, 2003, **125**, 314-315.
- 32 T. K. Sarma, D. Chowdhury, A. Paul and A. Chattopadhyay, *Chem. Commun.*, 2002, 1048-1049.
- 33 T. K. Sarma and A. Chattopadhyay, *J. Phys. Chem. A*, 2004, **108**, 7837-7842.
- 34 B. C. Sih and M. O. Wolf, *Chem. Commun.*, 2005, 3375-3384.
- 35 Y. Wang, Z. Liu, B. Han, Z. Sun, Y. Huang and G. Yang, *Langmuir*, 2005, **21**, 833-836.
- 36 S. K. Pillalamarri, F. D. Blum, A. T. Tokuhira and M. F. Bertino, *Chem. Mater.*, 2005, **17**, 5941-5944.
- 37 H. Tsuge, O. Natsuaki and K. Ohashi, *J. Biochem.*, 1975, **78**, 835-843.
- 38 W. Haiss, T. K. N. Thanh, J. Aveyard and D. G. Fernig, *Anal. Chem.*, 2007, **79**, 4215-4221.
- 39 S. K. Das, C. Dickinson, F. Lafir, D. F. Brougham and E. Marsilo, *Green Chem.*, 2012, **14**, 1322-1334.
- 40 H. Tsunoyama, H. Sakurai, N. Ichikuni, Y. Negishi and T. Tsutuda, *Langmuir*, 2004, **20**, 11293-11296.
- 41 Q. Liang, J. Liu, Y. Wei, Z. Zhao and M. J. MacLachlan, *Chem. Commun.*, 2013, **49**, 8928-8930.
- 42 D. Zaramella, P. Scrimin and L. J. Prins, *J. Am. Chem. Soc.*, 2012, **134**, 8396-8399.
- 43 R. Coppage, J. M. Slocik, H. R. Dakhel, N. M. Bedford, H. Heinz, R. R. Naik and M. R. Knecht, *J. Am. Chem. Soc.*, 2013, **135**, 11048-11054.
- 44 N. Zheng and G. D. Stucky, *J. Am. Chem. Soc.*, 2006, **128**, 14278-14280.
- 45 J. Zhang, B. Sun, X. Guan, H. Wang, H. Bao, Y. Huang, J. Qiao and G. Zhao, *Environ. Sci. Technol.*, 2013, **47**, 13011-13019.
- 46 J. C. Cruz, P. H. Pfromm, M. J. Tomich and M. E. Rezac, *Colloids Surf. B*, 2010, **81**, 1-10.
- 47 M. D. Gouda, S. A. Singh, A. G. A. Rao, M. S. Thakur and N. G. Karanth, *J. Biol. Chem.*, 2003, **278**, 24324-24333.
- 48 Z. Ma and H. Han, *Colloids Surf. A*, 2008, **317**, 229-233.
- 49 M. Colombo, S. Mazzucchelli, V. Colico, S. Avvakuvoka, L. Pandolfi, F. Corsi, F. Porta and Prosperi, *D. Angew. Chem. Int. Ed.*, 2012, **51**, 9272-9275.
- 50 C. A. Mirkin, *Inorg. Chem.*, 2000, **39**, 2258-2272.
- 51 H. J. Shin, I. W. Huang, Y. N. Huang, D. Kim, S. H. Han, J. S. Lee and G. Cho, *J. Phys. Chem. B*, 2003, **107**, 4699-4704.
- 52 W. Liu, J. Kumar, S. Tripathy, K. J. Senecal and L. Samuelson, *J. Am. Chem. Soc.*, 1999, **121**, 71-78.

## Table of Content (TOC)



Biogenic synthesis of Au nanoparticles and Au nanoparticle-polyaniline composite could be accomplished taking advantage of the reducing and catalytic activity of glucose oxidase.